2023 IEEE/ASME International Conference on Advanced Intelligent Mechatronics (AIM)
June 28-30, 2023. Seattle, Washington, USA

A Wheel to Leg Transformation Strategy in a Leg-Wheel Transformable Robot

Hua-Yu Wang, Liang-Jie Chen, Wei-Shun Yu and Pei-Chun Lin

***Abstract*—This study focuses on the wheel-to-leg transformation strategy of a leg-wheel transformable robot. The leg-wheel robot capable of fast transformation by 11-linkage mechanism has a leg length 3.4 times longer than its wheel radius. Because the robot in legged mode has fixed relative phases among the legs for locomotion, while the robot in wheeled mode has random phases owing to wheel steering, the transformation takes into account phase regulation. The transformation of a single leg-wheel is designed to minimize energy consumption to enable it to lift its body. The coordination of the leg-wheels during transformation is designed to maintain stability and prevent leg slippage in kinematic constraint. The proposed strategy was simulated and experimentally validated, and the results confirm its functionality.**

Keywords—Robot, Leg-wheel, transformation, modeling, kinematics, Webots

I. INTRODUCTION

Quadruped robots have proven to be a practical solution for use on challenging terrain. The high degree of freedom of legged morphology allows such robots to negotiate rough terrain effectively. Meanwhile, wheeled robots exhibit high mobility on flat terrain, move faster, and require less energy. By combining the advantages of these two locomotion systems, it is possible to deal with various types of complex terrain in a more efficient manner.

In the field of leg–wheel robots, the configuration of robots can be roughly divided into three types [1]. One type of robot has separate wheels and leg mechanisms. The second type has wheels located at the distal end of the legs, which perform a pure rolling motion, and a legged system is added when obstacle negotiation is required, such as obstacle climbing, jumping, active suspension, or skate-like motion. As an example of the first configuration, Airhopper [2] is a quadruped robot specialized for jumping. The leg system is driven by air pressure, and wheels with a smaller radius are added to the end points of the leg system. Usually, the wheels are used to move, and when encountering an obstacle, they drive the leg structure to take off and cross the obstacle. CENTAURO [3] is a four-legged robot with combined wheels and legs, which is equipped with a humanoid robot on the upper body to carry out more complex loading or repair tasks. [4] proposed how to switch from the homogeneous motion mode when the robot is moving. Anymal [5] , which has wheels at the end points of the feet, is a four-legged wheel-legged composite robot that exhibits high mobility in this configuration. Anymal [6] was originally a torque-controlled quadruped robot with four non-steerable torque control wheels, which allows a variety of motion patterns [7]. A motion plan was proposed for the mixed use of wheels and legs [8], representing a more dynamic solution for this type of robots. Additional examples of the second type are the TowrISIR [9], PAW [10] , and Mobile Robot [11].

This work is supported by National Science and Technology Council (NSTC), Taiwan, under contract MOST 110-2221-E-002-111-MY3.

The authors are with Department of Mechanical Engineering, National Taiwan University (NTU), No.1 Roosevelt Rd. Sec.4, Taipei 106, Taiwan. (Corresponding email: peichunlin@ntu.edu.tw).

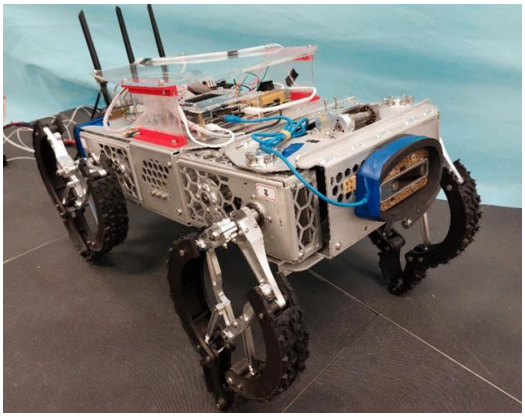

Fig. 1 A leg-wheel transformable robot with four linkage-based leg-wheel mechanism.

In the third type of robot, the wheel and leg can be transformed by the same mechanism. Wheel Transformer [12], a passive transformation robot, does not require an additional controller for the transformation process. When the wheel encounters an obstacle, it passively switches modes to overcome obstacles. OmniWheg [13] combines a Mecanum wheel with a connecting rod. The transformable wheel uses the characteristics of the Mecanum wheel to align the wheel before passing the obstacle. Previously, we have developed two generations of leg-wheel transformable robots. The first version, Quattroped [14] uses C-shape legs for transformation, and the second version, TurboQuad [15], has instant-change S-shaped legs and a CPG-based coordinated controller, which can achieve on-site transformation while the robot is in motion. The leg–wheel selection strategy has been studied analytically and experimentally as well [16]. Currently, we are developing the third generation of the leg-wheel transformation robot, as shown in Fig. 1. The robot is equipped with a novel linkage-based leg–wheel mechanism, whose leg length is 3.4 times of the wheel radius [17], achieving high ground clearance while the robot is in legged mode.

However, due to the morphological complexity of the leg-wheel, successful transformation requires coordination between all four leg-wheels. In this work, a leg–wheel transformation strategy is developed with the goal of quick and stable transformation, given any random configuration of all four wheels. The planned transformation avoids ground

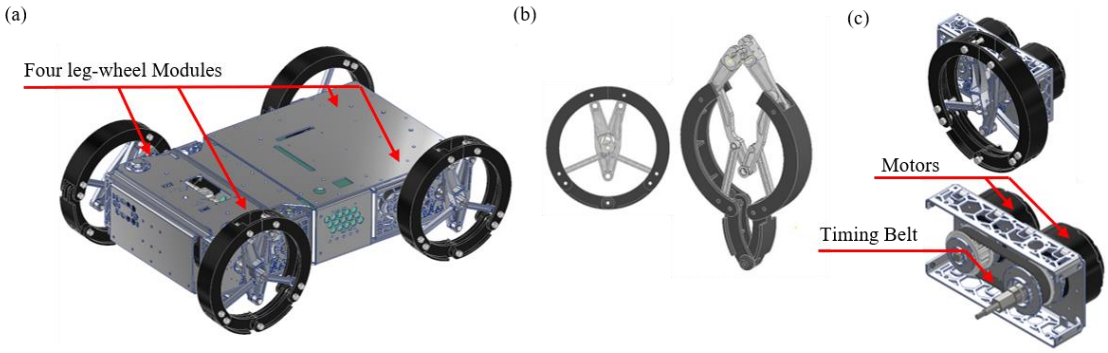

Fig. 2 (a) CAD drawing of the leg-wheel transformable robot; (b) CAD illustration of the leg-wheel mechanism; (c) CAD illustration of the 2-DOF driving module which provides 2-DOF coaxial and rotational output

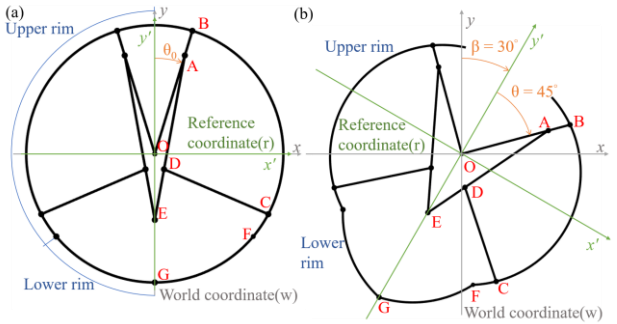

Fig. 3 . Notations of the leg-wheel when (a) in wheeled mode ($\beta = 0°$, $\theta_0 = 17°$) and (b) legged mode ($\beta = 30°$, $\theta = 45°$)

slippage and internal mechanical over-constraints among all legs, which may damage the mechanism and the actuators.

The remainder of this article is organized as follows. Section II briefly introduces the robot and the leg–wheel mechanism. Section III describes the trajectory planning of the leg–wheel, while motion coordination among all four leg–wheels is discussed in section IV. Section V reports on the simulation and experimental results, and Section VI concludes the work.

II. The Robot

The robot used in this research is the third-generation leg–wheel quadruped robot we developed. It is roughly the same as the previous two generations of robots, Quattroped and TurboQuad, both of which are equipped with four sets of modules that can quickly transform between wheels and legs. This robot has two modes, wheeled mode and legged mode, and accomplishes the wheel-to-leg transformation through a 2-DOF driving mechanism, as shown in Fig. 2(a).

The body of the robot is composed of folded aluminum plates, and four drive modules are embedded in the body. The electromechanical system and battery are installed in the middle and above the body. The front module is equipped with an Ackermann steering mechanism [18]. Table I summarizes the specifications of the robot.

The leg–wheel module[17] has two degrees of freedom, and the length of the leg pattern is about 3.4 times the radius of the wheel. The module configuration can be defined with two independent variables θ and β, as shown in Fig. 3. The symbol β represents the angle between the *y-axis* of the world coordinate and the symmetric line OG of the leg-wheel module, $180 \geq \beta > -180$. The symbol θ represents the angle between the *y-axis* of the reference coordinate and the right motor linkage OB of the leg-wheel module, $160 \geq \theta \geq 17$. The radius R of the leg–wheel module used by this robot is 100mm. In order to be able to withstand the weight of the robot and the impact force when it touches the ground while considering the goal of light weight, the connecting rod is made of aluminum and adopts an I-beam configuration. The wheel frame is reinforced with three-dimensional (3D) printing and added carbon fiber (see Fig. 2(b)).

TABLE I ROBOT SPECIFICATION

Weight	Body	20.985 kg
	Battery	0.22 kg
	Leg-Wheel(each)	0.7 kg
Body Dimensions	Width	0.33 m
	Length	0.62 m
	Height	13.4 cm
	Wheelbase	0.444m
Leg Dimensions	Wheel Diameter	0.20 m
	Max leg length	0.343 m

To drive the new leg–wheel mechanism, we have also developed a new driving module. Each leg–wheel mechanism on the robot has a 2-DOF drive module for driving and transformations. The mechanism achieves coaxial output through the timing belt and drives the left and right motor linkage angles separately, as shown in Fig. 2(c), so that the leg–wheel mechanism can change the leg length and posture arbitrarily on the sagittal plane. For more details, refer to [17]. The motor used in this module is Haitai's brushless motor HT-04. This motor has a lower gear ratio, and the continuous output torque also meets the needs of this quadruped robot.

III. Trajectory Planning of Each Leg-Wheel

As mentioned in section II, the states of the leg are parametrized by two independent variables, θ and β. Since a given hip point position (point O) will correspond to multiple feasible (β,θ) combinations, it is not possible to use the reverse kinematics to directly plan trajectories. Therefore, this study uses forward kinematics to plan the shape changes of (β,θ) in joint space. The trajectory planning involves two steps. First, the trajectories initially planned by polynomial functions are filtered to discard undesired motion patterns. Second, the best

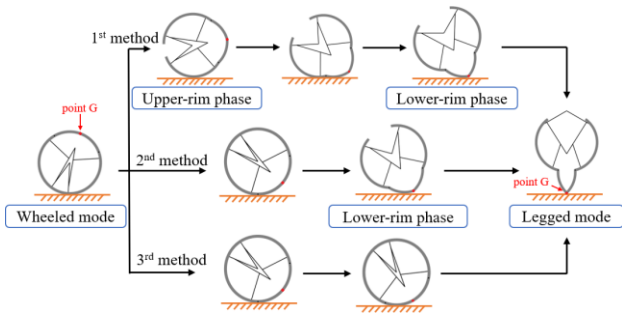

Fig. 4 Methods of wheel-to-leg transformation. The 1st method starts transforming the leg-wheel from its upper-rim phase. The 2nd method transforms the leg-wheel from its lower-rim phase. The 3rd method transforms the leg-wheel only when point G comes in contact with the ground.

trajectory is selected based on energy efficiency during the wheel-to-leg transformation of the robot.

This leg–wheel module has three methods to switch from wheeled mode to legged mode, as shown in Fig. 4. The first is transformation from the upper-rim phase. The advantage of this method is that it has a longer time duration for switching. The disadvantage is that the center of rotation abruptly changes while the ground contact point switches from the upper-rim to the lower-rim. Thus, the motion of the O point (i.e., hip point of the robot) is not smooth. The second method is to start switching from the lower rim. In this case, when the leg–wheel module rolls to the end of the lower rim, it switches to point contact, and the movement of point O is continuous. The third method is to switch when point G touches the ground. However, with this method, the leg extension speed needs to be faster than the rolling speed, or the contact point will switch from one side of the lower rim to the other side. After comprehensive consideration, the second method is adopted.

The wheeled mode is a state in which β is constantly changing and θ is maintained at θ_0 for this wheel leg–wheel module. We need to choose an operating point β_{start} where the wheel mode will start to change and specify an end point β_{end} to plan the trajectory between two points. During the transformation process, θ must be changed from θ_0 to the required angle based on the length of the leg that is needed. The β operating range of the entire lower rim is -50° to 0°. To prevent the upper rim from interfering with the transformation movement during operation, we choose $\beta_{start} = -45°$ as the operating point for starting the transformation, and we set the end point of deformation as $\beta_{end} = 0°$, for reasons we will mention in section IV. The calculation here is based on the standard length of the leg pattern of 200mm, so we can get the following boundary conditions: $\beta_{start} = -45°$, $\beta_{end} = 0°$; $\theta_{start} = 17°, \theta_{end} = 74.5°$.

With the boundary conditions mentioned above, trajectory planning can be carried out. We apply these two variables to the linear, quadratic, and cubic functions, respectively, and combine them as the operation trajectory of the leg–wheel module. For quadratic functions, we give additional points at the midpoint of time (β_{mid} ,or θ_{mid}), and for cubic functions we give additional points at 1/3 and 2/3 of the timeline (β_{mid1}, β_{mid2},or θ_{mid1}, θ_{mid2}). In this case, the length of the timeline is 1 second. However, the length of the timeline will be scaled proportionally depending on the wheeled mode velocity. We try a large number of additional points between the start points and the end points. Then, we use forward kinematics to calculate the trajectories and record them all.

The method we use is similar to [17]. The trajectory planning is carried out according to the combination of the functions and boundary conditions. Applying β and θ to the linear, quadratic, and cubic functions, there will be a total of nine combinations. The details of the trajectories under all combinations can refer to [17]. However, the difference is that the purpose of [17] is to make a single module take off, and the focus is on the speed and direction when it leaves the ground, so there are various boundary conditions that can achieve the goal. This research needs to focus on the stability and efficiency of transformation, and one purpose will only correspond to one boundary condition. The filter criteria will also be different.

With these trajectories, we are going to perform the first filtering. It is expected that the robot moves toward the target, so first we remove the trajectory with a negative speed in the *x* direction and *y* direction. Then, we hope that the whole transformation process will have a close to constant speed because the legs of this mechanism are much longer than the radius of the wheel. If the speed changes too drastically, the robot will be very unstable. Therefore, we screen the x-direction velocity and y-direction velocity of the trajectory and select the smallest standard deviation of these two features to initially reduce the trajectory, as shown in Fig. 5.

The jerk cost function is utilized as the second-step trajectory selection. The cost function is designed as follows:

$$C = \int_0^T J_{L\_motor}^2 + J_{R\_motor}^2 \, dt \tag{1}$$

where J_{L_motor} is the result of differentiating the motor angel ϕ_R trajectory three times, and J_{R_motor} has the same relationship with motor angel ϕ_L.

The jerk analysis[19] is mainly to optimize the output change of the two motors. If there is no drastic acceleration change, the motor does not need to waste much energy to resist inertia. In practice, more acceleration changes may magnify hardware defects, such as motor clearance or manufacturing tolerances, so we use this cost function to filter out the final trajectory. The trajectory with the minimum of *C* will be the solution for the wheel-to-leg trajectory. In order to use this cost function, we need to convert (β,θ) into the parameters used by the motor (ϕ_R, ϕ_L). Mapping between two coordinates is performed as follows:

$$\begin{bmatrix} \phi_R \\ \phi_L \end{bmatrix} = \begin{bmatrix} 1 & 1 \\ -1 & 1 \end{bmatrix} \begin{bmatrix} \theta \\ \beta \end{bmatrix} \tag{2}$$

After transforming the coordinates of the previously selected trajectories and applying them to the cost function, the trajectories used for the transformation of the leg-wheel module can be obtained as:

$$\begin{cases} \theta = 58.1633t + 15.8367 \\ \beta = -28.9966t^2 + 75.495t - 46.4983 \end{cases} \tag{3}$$

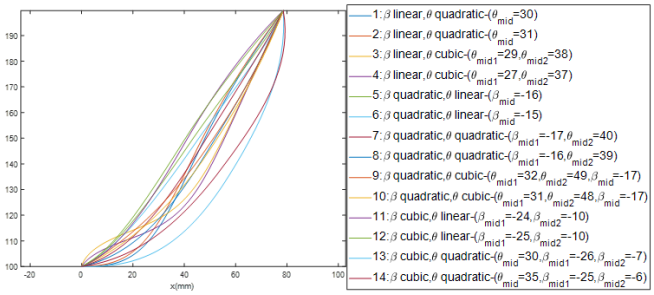

Fig. 5 Selected trajectories in these combinations for optimization.

IV. Motion Coordination Among All Four Leg-Wheels for Wheel-to-Leg Transformation

With the designed wheel-to-leg transformation trajectories mentioned above, we are going to coordinate the timing of the transformations of the four leg-wheel modules on this robot. The left front module is marked as $module_{lf}$, the right front module is $module_{rf}$, the right rear one is $module_{rh}$ and the left rear one is $module_{lh}$. In order to control these four modules in wheeled mode, each module corresponds to one symbol β_i $(i = lf, rf, rh, lh)$.

The robot operated in wheeled mode does not have fixed relative phases of the leg–wheel when the turning motion is involved. Thus, when the wheel-to-leg transformation is to be initiated, the phases of the wheels may be random, and the developed strategy should be functional with any β_i. In order to align the β_i of the four wheels to enter the legged mode, we propose the following method. In wheeled mode, first transform the front two legs. The front leading leg transforms first, and another front leg transforms immediately after leaving the ground. Keep the front two modules in the legged mode and the rear two modules in the wheeled mode (mixed mode) until the rear wheels enter the phase that can carry out the transformation. Then, the rear leading leg makes the switch, and the other rear leg transforms immediately after leaving the ground. Finally complete the entire transformation process. Using this method, it is possible to perform the wheel-to-leg transformation while aligning the four wheels β_i without any slippage or deflection of the robot. The entire transformation process is shown in Fig 6.

It should be noted that since we want the entire transformation process to be constant, we only need to ensure that the center of mass is projected on the supporting polygon during the entire process. The mass center of our robot is in the middle of main body, which is why we set the transformation end point β_{end} at 0° degrees in section III. When the robot's front modules are in legged mode and the rear modules are in wheeled mode, if the β of the front foot exceeds 0°, the center of mass will be projected outside the support polygon. When the rear modules are transforming, the front legs must also move from β=0° to ensure the stability of the robot.

Next, we will explain how to assign the movements of each set of wheel–leg modules throughout the transformation process. We use an algorithm with a weight function to plan the entire progress. This method requires knowledge of the current state of the robot, including the wheeled mode β_i $(i = lf, rf, rh, lh)$, forward speed V, legged mode step length L_{step}, and standing height H_{stance}. Based on this information, three parameters can be calculated. After these parameters are standardized and put into the weight function, the front and rear leading legs and the robot's motion plan during the transformation process will be obtained. The weight function is as follows:

$$G = w_1 \times D_{initial} + w_2 \times N_{step} + w_3 \times E_{step\ length} \quad (4)$$

with the weights $w1 + w2 + w3 = 1$, The transformation process with the minimum of G calculated by this equation is the actual solution.

1) Initial distance: Calculating the distance from the current phase of the two front legs (β_{lf}, β_{rf}) to β_{start} and divide by the circumference of the wheel to normalize, we can get $D_{initial}$.

$$D_{initial} = \frac{(\beta_i - \beta_{start})}{2\pi R} \quad (5)$$

2) Step counts: When the front legs transform, the rear wheel will roll forward at the same time. Because the trajectory is pre-calculated in Section III, the rear wheels beta after the transformation of the front wheel $(\beta_{lh,1st\ tr}, \beta_{rh,1st\ tr})$ can be calculated. In this way, four leading foot combinations will be obtained: the left front leg to the left rear leg, the left front leg to the right hind leg, the right front leg to the left rear leg, and the right front leg to the right rear leg. By calculating

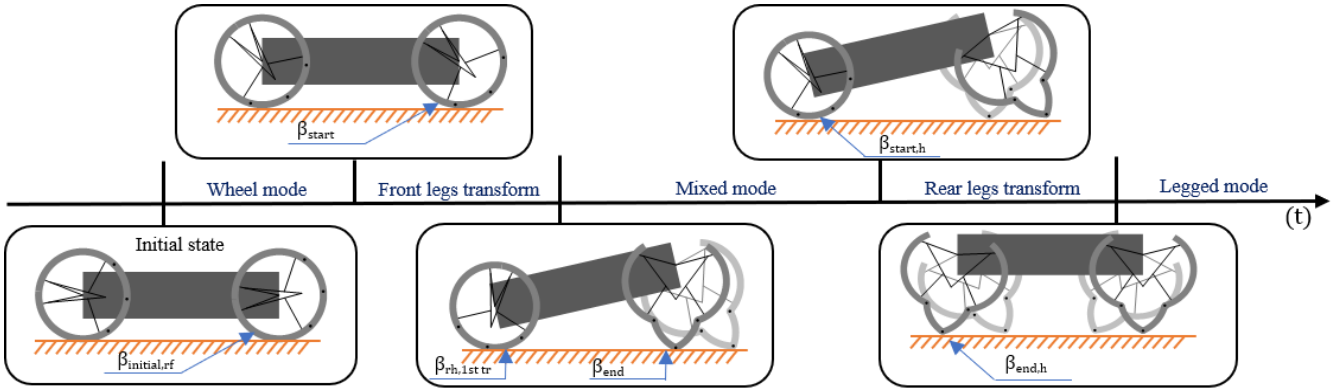

Fig. 6 Timeline of the entire leg-wheel transformation process. In the figure, the right front and right rear legs are selected as leading legs. The symbols βi needed in each period are marked.

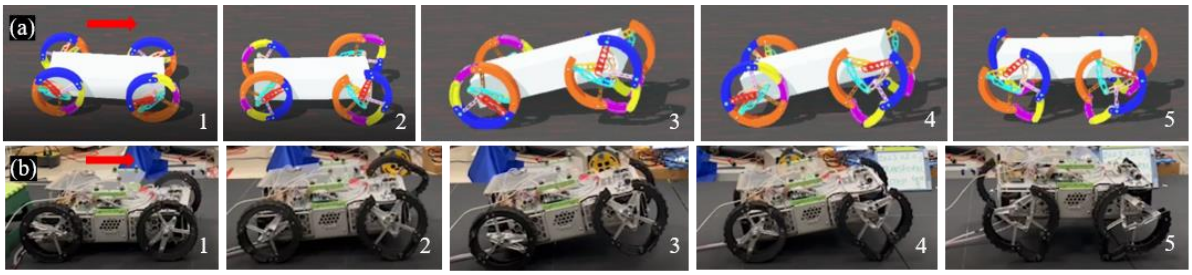

Fig. 7. Snapshots of the robot in (a) simulation and (b) experiment during the leg-wheel transformation process. The numbers of the subfigures represent the sequences. 1) Initially, the robot driven in wheeled mode has random leg-wheel phases. 2) The right front leg-wheel starts to transform. 3) The two front legs are transformed into legged mode with correct relative phases. 4) The left rear leg rotates to βstart,hind first, and it is selected as the rear leading leg for transformation. 5) The leg-wheel transformation of the robot is completed. The video of the robot in transformation can be found in https://www.youtube.com/watch?v=X4iWha308Lk&feature=youtu.be

the number of steps required according to the β_i difference of each combination (N'_{step} ,which has to be positive integer) and dividing by the number of steps required to walk the circumference of the wheel to normalize, we can get N_{step}.

$$N'_{step} = round\left(\beta_{i,1st\ tr} - \beta_{start,h}/L_{step}\right) \quad (6)$$

$$N_{step} = \frac{N'_{step}}{2\pi R/L_{step}} \quad (7)$$

3) Step Length error: As mentioned earlier, after calculating the number of steps required N'_{step}, we can know the difference between the step length and the legged mode step length L_{step}. By dividing the length of the legged mode step length to normalize, we can get $E_{step\ length}$. The weight of this parameter can be adjusted according to the terrain conditions or the gaits after the transformation. However, since there is currently no reference terrain condition, we set this weight very small.

$$E_{step\ length} = \frac{N'_{step} \times R/\left(\beta_{i,1st\ tr} - \beta_{start,h}\right) - L_{step}}{L_{step}} \quad (8)$$

V. Experiment

The proposed strategy is simulated in Webot[20] and experimentally evaluated. A motion capture system (Vicon) is utilized to capture the motion of the robot.

A. Validation filter method of trajectories

In section III, we used a cost function as the final way to filter the trajectory. In this experiment, we implemented the 14 trajectories that were initially filtered and average the data to see if the trajectory with the lowest energy consumption is the same as we determined in section III. We use the same trajectory for both front legs of the robot and compare them to each other.

It can be observed from the TABLE II that trajectory number 4 consumes the most energy (*92.454 Joule*), which is the combination of (β linear, θ cubic). When this combination is put into the cost function used earlier, the result is also the worst, so the experimental results here are consistent with the theoretical values. The combination of (β quadratic, θ linear) consumes relatively little energy, and trajectory number 5 ($\beta_{mid} = -16$) consumes the least energy (*88.459 Joule*). This trajectory is exactly the result we calculated with the cost function (3) earlier. However, since these trajectories have been screened for the first time and the extremely energy-intensive trajectories have been shaved, there is no huge difference in terms of energy consumption.

TABLE II Power Consumptions of the robot using different leg-wheel trajectories

List of Trajectories			Power consumption (Joule)
No.	*Combination*	*Additional point(s)*	
1	β linear θ quadratic	$\theta_{mid} = 30°$	90.385
2		$\theta_{mid} = 31°$	90.545
3	β linear θ cubic	$\theta_{mid1} = 29°, \theta_{mid2} = 38°$	91.697
4		$\theta_{mid1} = 27°, \theta_{mid2} = 37°$	92.454
5	β quadratic θ linear	$\beta_{mid} = -16°$	88.459
6		$\beta_{mid} = -15°$	88.815
7	β quadratic θ quadratic	$\beta_{mid} = -17°, \theta_{mid} = 40°$	90.16
8		$\beta_{mid} = -16°, \theta_{mid} = 39°$	90.186
9	β quadratic θ cubic	$\beta_{mid} = -17°$, $\theta_{mid1} = 32°, \theta_{mid2} = 49°$	90.735
10		$\beta_{mid} = -17°$, $\theta_{mid1} = 31°, \theta_{mid2} = 48°$	90.698
11	β cubic θ linear	$\beta_{mid1} = -24°, \beta_{mid2} = -10°$	90.993
12		$\beta_{mid1} = -25°, \beta_{mid2} = -10°$	90.984
13	β cubic θ quadratic	$\beta_{mid1} = -26°, \beta_{mid2} = -7°$ $\theta_{mid} = 30°$	90.957
14		$\beta_{mid1} = -25°, \beta_{mid2} = -6°$ $\theta_{mid} = 35°$	91.09

B. Simulation of transformation process

In Webot, we randomly give the initial state of the robot, hoping that the robot will perform leg–wheel transformation in the current state. Fig. 7(a) shows the transformation process of one of the states. Here, the initial states of the angle of the four wheels are ($\beta_{lf} = 47.6°, \beta_{rf} = -144.9°, \beta_{rh} = -79.7°, \beta_{lh} = 16.8°$), the wheeled mode speed is 40mm/s and the legged mode step length L_{step} is 120mm. The robot transforms with the right front leg and the left rear leg as the leading legs. Then, the robot takes two steps in leg–wheel mixed mode. Finally, the robot successfully transforms to foot mode.

C. Test of transformation process

We randomly select many initial states to test on the robot and use Vicon to capture the dynamics of the robot. The test results are shown in Fig. 7(b). The initial state of this experiment uses the same data as in section V-B. We will observe whether the robot slips or deflects during the whole process. Fig. 8 presents the difference between the ideal

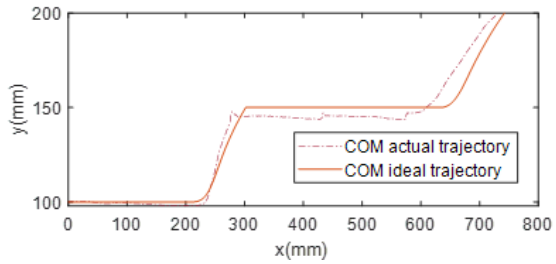

Fig. 8 The ideal and the actual trajectories of the initial state as follow: $\beta_{lf} = 47.6°, \beta_{rf} = -144.9°, \beta_{rh} = -79.7°, \beta_{lh} = 16.8°$.

trajectory of the robot and the actual trajectory in this experiment.

In the initial state, the robot needs to take two steps in leg–wheel mixed mode. After calculation, the ideal forward distance of the robot is 742mm, while the actual forward distance of the robot is 727mm. The deflection in the *z-axis* direction is less than 12mm, meaning that almost no deflection occurs. However, there is slight slippage in leg–wheel mixed mode. We can observe that at mixed mode, there are two bumps on the actual trajectory. Because of the reaction force of the leg touching the ground, the robot is a little unstable, so there is slight slippage.

Based on previous experimental experience, we know that if the robot slips, the actual distance advanced is less than the ideal value. In these experiments, the performance of the actual trajectory in the *x-axis* direction is only about 6% less than the theoretical value. The offset in the *z-axis* direction is small enough to ignore. Moreover, the deviation of the robot in the *z-axis* direction is so small that it can also be ignored, confirming the advantage of this method.

VI. Conclusion and Future Work

We report on the development of a wheel-to-leg transformation strategy, which allows the robot to transform its morphology from wheeled mode to legged mode with any initial wheeled configuration and without slippage during transformation. The deployed cost function can effectively select suitable trajectories with low power consumption. The algorithm for coordination among four leg-wheels can yield feasible transformation strategy in various initial states, simultaneously aligning the four wheels and transforming from wheeled to legged mode. Experimental results confirm that the robot can transit successfully.

In the future, we hope to add the function of vision so that the robot can determine the height after transformation and the coefficient configuration in the algorithm according to the terrain. The current method does not allow the rear foot to intervene in the transformation process of the front foot. We expect to complete this algorithm to provide more diverse and efficient conversion processes to cope with various situations.

Reference

[1] F. Michaud *et al.*, "Multi-Modal Locomotion Robotic Platform Using Leg-Track-Wheel Articulations," *Autonomous Robots,* vol. 18, no. 2, pp. 137-156, 2005/03/01 2005, doi: 10.1007/s10514-005-0722-1.

[2] T. Tanaka and S. Hirose, "Development of leg-wheel hybrid quadruped "AirHopper" design of powerful light-weight leg with wheel," in *2008 IEEE/RSJ International Conference on Intelligent Robots and Systems*, 22-26 Sept. 2008 2008, pp. 3890-3895, doi: 10.1109/IROS.2008.4650880.

[3] N. Kashiri *et al.*, "CENTAURO: A Hybrid Locomotion and High Power Resilient Manipulation Platform," *IEEE Robotics and Automation Letters,* vol. 4, no. 2, pp. 1595-1602, 2019, doi: 10.1109/LRA.2019.2896758.

[4] T. Klamt *et al.*, "Supervised Autonomous Locomotion and Manipulation for Disaster Response with a Centaur-Like Robot," in *2018 IEEE/RSJ International Conference on Intelligent Robots and Systems (IROS)*, 1-5 Oct. 2018 2018, pp. 1-8, doi: 10.1109/IROS.2018.8594509.

[5] M. Bjelonic *et al.*, "Keep Rollin'—Whole-Body Motion Control and Planning for Wheeled Quadrupedal Robots," *IEEE Robotics and Automation Letters,* vol. 4, no. 2, pp. 2116-2123, 2019, doi: 10.1109/LRA.2019.2899750.

[6] M. Hutter *et al.*, "ANYmal - a highly mobile and dynamic quadrupedal robot," in *2016 IEEE/RSJ International Conference on Intelligent Robots and Systems (IROS)*, 9-14 Oct. 2016 2016, pp. 38-44, doi: 10.1109/IROS.2016.7758092.

[7] V. S. Medeiros, E. Jelavic, M. Bjelonic, R. Siegwart, M. A. Meggiolaro, and M. Hutter, "Trajectory Optimization for Wheeled-Legged Quadrupedal Robots Driving in Challenging Terrain," *IEEE Robotics and Automation Letters,* vol. 5, no. 3, pp. 4172-4179, 2020, doi: 10.1109/LRA.2020.2990720.

[8] M. Bjelonic, P. K. Sankar, C. D. Bellicoso, H. Vallery, and M. Hutter, "Rolling in the Deep – Hybrid Locomotion for Wheeled-Legged Robots Using Online Trajectory Optimization," *IEEE Robotics and Automation Letters,* vol. 5, no. 2, pp. 3626-3633, 2020, doi: 10.1109/LRA.2020.2979661.

[9] W. Du, M. Fnadi, and F. Benamar, "Rolling based locomotion on rough terrain for a wheeled quadruped using centroidal dynamics," *Mechanism and Machine Theory,* vol. 153, p. 103984, 2020.

[10] J. A. Smith, I. Sharf, and M. Trentini, "PAW: a hybrid wheeled-leg robot," in *Proceedings 2006 IEEE International Conference on Robotics and Automation, 2006. ICRA 2006.*, 2006: IEEE, pp. 4043-4048.

[11] H. Jiang, G. Xu, W. Zeng, and F. Gao, "Design and kinematic modeling of a passively-actively transformable mobile robot," *Mechanism and Machine Theory,* vol. 142, p. 103591, 2019.

[12] Y. S. Kim, G. P. Jung, H. Kim, K. J. Cho, and C. N. Chu, "Wheel Transformer: A Wheel-Leg Hybrid Robot With Passive Transformable Wheels," *IEEE Transactions on Robotics,* vol. 30, no. 6, pp. 1487-1498, 2014, doi: 10.1109/TRO.2014.2365651.

[13] R. Cao, J. Gu, C. Yu, and A. Rosendo, "OmniWheg: An Omnidirectional Wheel-Leg Transformable Robot," in *2022 IEEE/RSJ International Conference on Intelligent Robots and Systems (IROS)*, 23-27 Oct. 2022 2022, pp. 5626-5631, doi: 10.1109/IROS47612.2022.9982030.

[14] S. C. Chen, K. J. Huang, W. H. Chen, S. Y. Shen, C. H. Li, and P. C. Lin, "Quattroped: A Leg--Wheel Transformable Robot," *IEEE/ASME Transactions on Mechatronics,* vol. 19, no. 2, pp. 730-742, 2014, doi: 10.1109/TMECH.2013.2253615.

[15] W. H. Chen, H. S. Lin, Y. M. Lin, and P. C. Lin, "TurboQuad: A Novel Leg–Wheel Transformable Robot With Smooth and Fast Behavioral Transitions," *IEEE Transactions on Robotics,* vol. 33, no. 5, pp. 1025-1040, 2017, doi: 10.1109/TRO.2017.2696022.

[16] T. H. Wang and P. C. Lin, "A Reduced-Order-Model-Based Motion Selection Strategy in a Leg-Wheel Transformable Robot," *IEEE/ASME Transactions on Mechatronics,* vol. 27, no. 5, pp. 3315-3321, 2022, doi: 10.1109/TMECH.2021.3126606.

[17] H.-Y. Chen, T.-H. Wang, K.-C. Ho, C.-Y. Ko, P.-C. Lin, and P.-C. Lin, "Development of a novel leg-wheel module with fast transformation and leaping capability," *Mechanism and Machine Theory,* vol. 163, p. 104348, 2021/09/01/ 2021, doi: https://doi.org/10.1016/j.mechmachtheory.2021.104348.

[18] R. N. Jazar, "Steering Dynamics," in *Vehicle Dynamics: Theory and Application*, R. N. Jazar Ed. Boston, MA: Springer US, 2008, pp. 379-454.

[19] A.-N. Sharkawy, "Minimum Jerk Trajectory Generation for Straight and Curved Movements: Mathematical Analysis," *arXiv preprint arXiv:2102.07459,* 2021.

[20] J. Collins, S. Chand, A. Vanderkop, and D. Howard, "A Review of Physics Simulators for Robotic Applications," *IEEE Access,* vol. 9, pp. 51416-51431, 2021, doi: 10.1109/ACCESS.2021.3068769.